Cathodoluminescence of undoped and Si-doped ε-Ga_2O_3 films

V.Montedoro[a], A.Torres[c], S.Dadgostar[c], J.Jimenez[c], M.Bosi[b], A.Parisini[a], R.Fornari[ab]

a *Dept. of Mathematical, Physical and Computer Sciences, University of Parma, Viale delle Scienze 7/A, 43124 Parma, Italy*
b *Institute of Materials for Electronics and Magnetism (IMEM-CNR), Viale delle Scienze 37/A, 43124 Parma, Italy*
c *Dept. of Condensed Matter Physics, University of Valladolid, Paseo de Bel´en 19, 47011 Valladolid, Spain*

Abstract

Cathodoluminescence (CL) investigations are performed on nominally undoped and Si-doped ε-Ga_2O_3 samples grown by metal-organic vapor phase epitaxy on (0001)-Al_2O_3 substrates, using different carrier gases. All films exhibit a broad low-temperature CL emission extending over the photon energy range 2–3.4 eV. Emission deconvolution suggests that four narrower bands centered at about 2.4, 2.75, 3.0 and 3.15 eV may well account for the broad band. While the position of these peaks results independent of the growth conditions, significant intensity differences are observed. A general reduction of the broad emission is evidenced as the Si concentration increases. No band-to-band recombination is observed. Temperature dependence of the CL signal shows a trend consistent with radiative transitions from the CB to deep acceptor states, probably of intrinsic nature.

Keywords: Gallium oxide, Wide bandgap semiconductors, Cathodoluminescence, Deep levels

1. Introduction

Among wide band-gap oxide semiconductors, Ga_2O_3 is attracting much attention as an interesting candidate for the fabrication of power transistors and optoelectronic devices, such as solar-blind UV detectors [1], [2], [3], [4], [5], [6], [7]. The band gap of 4.6–4.9 eV and an estimated breakdown electric field of 8 MV/cm make it one of the most promising transparent semiconducting oxides (TSO) [8]. There are several polymorphs of gallium oxide (α, β, ε, δ, γ), but the β-phase (4.9 eV bandgap) is the most studied one because it is thermodynamically stable. Furthermore, it can be grown from the melt as a single crystal suitable for the production of substrates [9], [10], [11]. However, it presents also some disadvantages, such as considerable optical and thermal anisotropy [12], and a strong cleavage tendency along the planes (1 0 0) and (0 0 1).

The second most stable phase is believed to be the ε-phase (bandgap around 4.6 eV) [4], with a pseudo-hexagonal crystal structure (orthorhombic with 120° oriented domains, also referred to as κ) [13]. It is thermodynamically stable up to 700 °C, and it undergoes a complete transition to β-phase at temperatures higher than 900 °C [14]. First results concerning the electrical properties of ε-Ga_2O_3 showed that epitaxial films can be successfully doped with silicon and tin to get resistivity down to about 1 Ωcm [15]. Furthermore, ε-Ga_2O_3 possesses higher crystallographic symmetry than the β-polymorph, it can be deposited on different substrates and shows an interesting ferroelectric behavior [16], [17], [18].
The β-phase has been extensively investigated by cathodoluminescence (CL), photoluminescence (PL), deep-level transient spectroscopy (DLTS), deep-level optical spectroscopy (DLOS) [19], [20], [21], [22], [23], in order to detect deep levels and related optical transitions, however, such information is not yet available for ε-Ga_2O_3. In this work, temperature-dependent cathodoluminescence (CL) measurements were applied for the first time to study epitaxial ε-Ga_2O_3 layers grown under different conditions and differently doped. It was observed that generally the films present a broad emission band extending over the 2–3.4 eV photon energy range, which we ascribed to the convolution of four partially overlapping bands. The relative intensity of the four bands changes with the growth parameters and the dopant concentration, as well as with the measurement temperature. The nature of the deep levels is discussed considering available electrical data from previous investigations. This is the first investigation on radiative deep levels in ε-Ga_2O_3 and their dependence on doping and growth conditions.

2. Experimentals

Undoped and silicon-doped ε-Ga_2O_3 films were grown on c-oriented sapphire substrates by MOVPE in a low-pressure reactor at 600°-650 °C. Trimethylgallium (TMG) and ultrapure water, stored in stainless steel bubblers at 1 °C and 30 °C, respectively, were used as precursors, using H_2, He, or N_2 as carrier gas. The ratio of their partial pressures (oxygen-to-gallium) was in the range 200–350. For Si-doped films, SiH_4 diluted 0,05% in H_2 was injected into the reactor via the TMG line to get effective silane fluxes between 0,001–0,05 sccm. A list of the samples studied in the present work is reported in Table 1.

Table 1. Growth parameters and properties of the analyzed samples.

Sample number and SiH_4 flow (sccm)	**T(°C) – P (mbar)**	**Carrier flux (sccm)**	**Carrier gas**	**Thickness (nm)**	**Time (min)**	**O/Ga ratio**
#341/Undoped	610–72	2000	N_2	250–350	120	242
#342/0.005 sccm (SiH_4)	600–80	2000	N_2	450	120	218
#344/0.001 sccm (SiH_4)	600–80	2000	N_2	350	120	218
#348/0.0125 sccm (SiH_4)	610–75	2000	N_2	800	120	233
#395/Undoped	610–60	2000	H_2	280	15	349
#425/Undoped	610–60	2000	H_2	6000	320	349
#426/0.005 sccm (SiH_4)	610–60	2000	H_2	1000	60	349
#430/0.0125 sccm (SiH_4)	610–60	2000	H_2	1000	60	349
#431/0.05 sccm (SiH_4)	610–60	2000	H_2	900	60	349
#479/Undoped	650–100	400	He	200	17	206

Epitaxial films with thickness ranging from 0.5 μm to 5 μm were selected and tested by X-ray diffraction in order to check their ε-phase purity. Fig. 1a shows the X-ray diffraction pattern recorded using the Cu Kα radiation for a Si-doped layer grown using H_2 carrier gas, sample #430. The shift of spectra of ε-Ga_2O_3 layers with respect to those of β-Ga_2O_3 has been pointed out in Ref. [24], also evidencing a perfect correspondence in angle between peaks of equal Miller indexes of nominally undoped and Si-doped ε-Ga_2O_3 layers. The optimum crystallographic quality of the ε-Ga_2O_3 layers is confirmed in all the spectra by the small linewidth of the peaks which permits to resolve the splitting due to Kα1 and Kα2 radiations, without any broadening of the peaks due to doping. To highlight this result, in Fig. 1b, the split (0 0 0 6) peak of Fig. 1a is compared with the corresponding diffraction peak of an undoped layer, grown using H_2, showing the full overlap of the spectra.

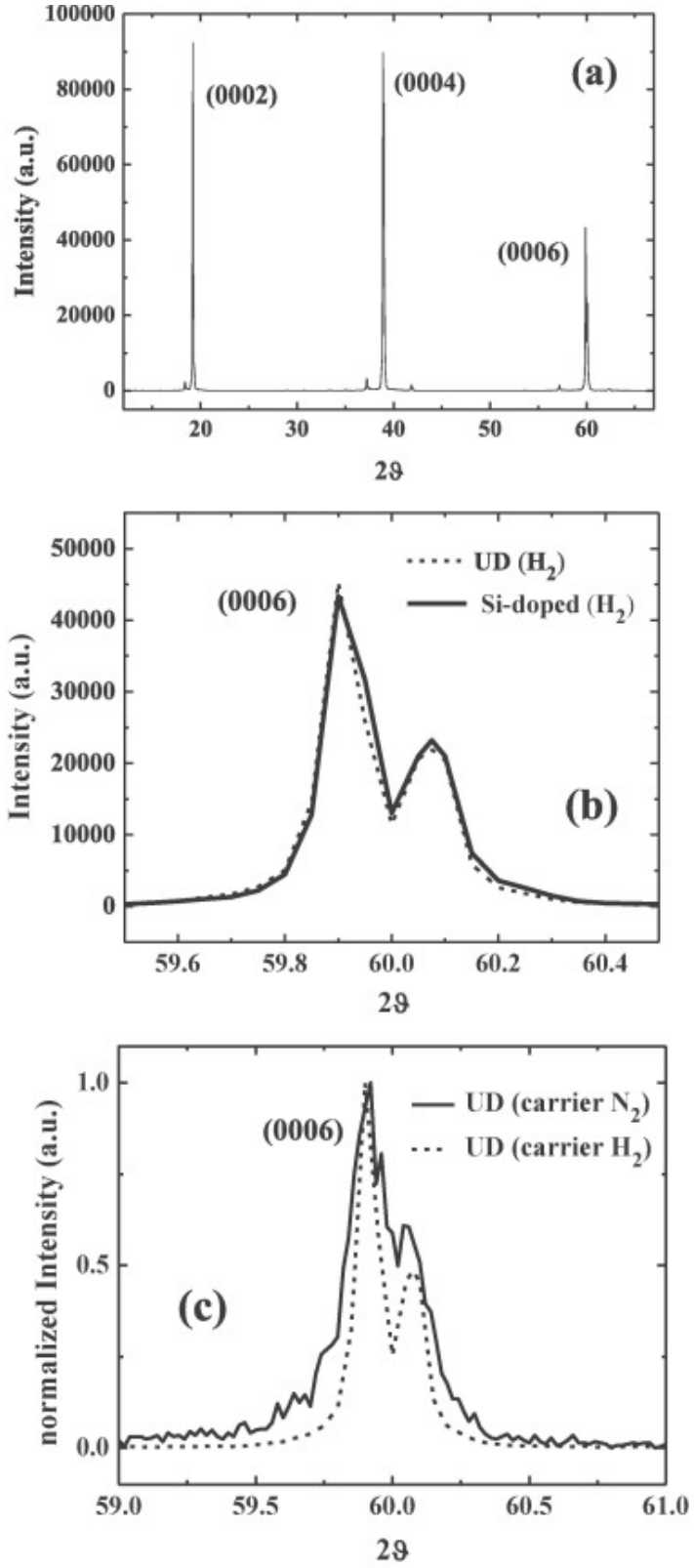

Fig. 1. (a) X-ray-diffraction pattern of #430 Si-doped epitaxial layer. (b) Comparison between the Kα1-Kα2 split (0 0 0 6)-peaks of sample #430 (continuous line) and of an undoped ε-Ga_2O_3 sample grown with H_2 carrier gas (dashed line). (c) Comparison between the (0 0 0 6) peaks of an undoped sample grown either using N_2 (continuous line) and H_2 (dashed line) carrier gas.

This result supports the hypothesis of a uniform incorporation of Si atoms as isolated donors in the doped layers, as proposed in Refs. [15], [24], without formation of precipitates or other extended defects. The crystallographic quality was poorer when N_2 carrier gas was used instead of H_2, as shown in Fig. 1c.

The CL study was carried out with a MonoCL2 system from Gatan UK, attached to a field-emission scanning electron microscope (FESEM-LEO 1530). The detector for the spectral analysis was a Peltier-cooled CCD, while a photomultiplier was used for recording panchromatic CL images. CL spectra were acquired at 80 K for every sample, while temperature dependence investigation, from 80 K to 280 K, was also performed on a few selected samples. The e-beam energy was varied between 5 and 30 KeV. The penetration depth, estimated from Montecarlo simulation by means of Casinosoftware [25], in Ga_2O_3 at 5 kV is ≈270 nm, with maximum energy loss at around 81 nm, whereas the penetration depth at 30 kV is ≈4 μm, with maximum loss energy around 1.3 μm. The samples were not coated, since no significant specimen charging effect was observed under the experimental conditions used.

3. Results and discussion

Typical CL spectra from a set of nominally undoped ε-Ga_2O_3 epilayers at 80 K are shown in Fig. 2a, while Fig. 2b reports the CL spectrum of a thick layer (5 μm). For this high thickness there are no luminescence contributions from the sapphire substrate even when high-energy electron beams are used in order to enhance the signal to noise ratio. No band-to-band or excitonic transitions were observed. The spectrum of Fig. 2b, consists of a broad band in the spectral range 2–3.4 eV that may be deconvoluted and satisfactorily fitted by four Gaussian bands centered at 2.4 eV (517 nm: A), 2.75 eV (450 nm: B), 3.0 eV (413 nm: C), and 3.15 eV (394 nm: D). It is worth noting that with the four-Gaussian approach we were able to fit all the spectra, independently of the sample. The intensity of peak D is appreciable only in few samples, while it is actually negligible in most of them, independently of the carrier gas, consistently with the data shown in Ref. [4]. See e.g. Fig. S1 in Supplementary information and Fig. 7b discussed below. To be noted, that in case of negligible peak D, the fitting of emissions is in principle possible with just three peaks: the spectral position of A, B, C bands does not change appreciably, while their FWHM increase. This speaks in favor of a general four peak-based deconvolution procedure, that can provide a reliable estimate of positions of the corresponding deep levels in all cases.

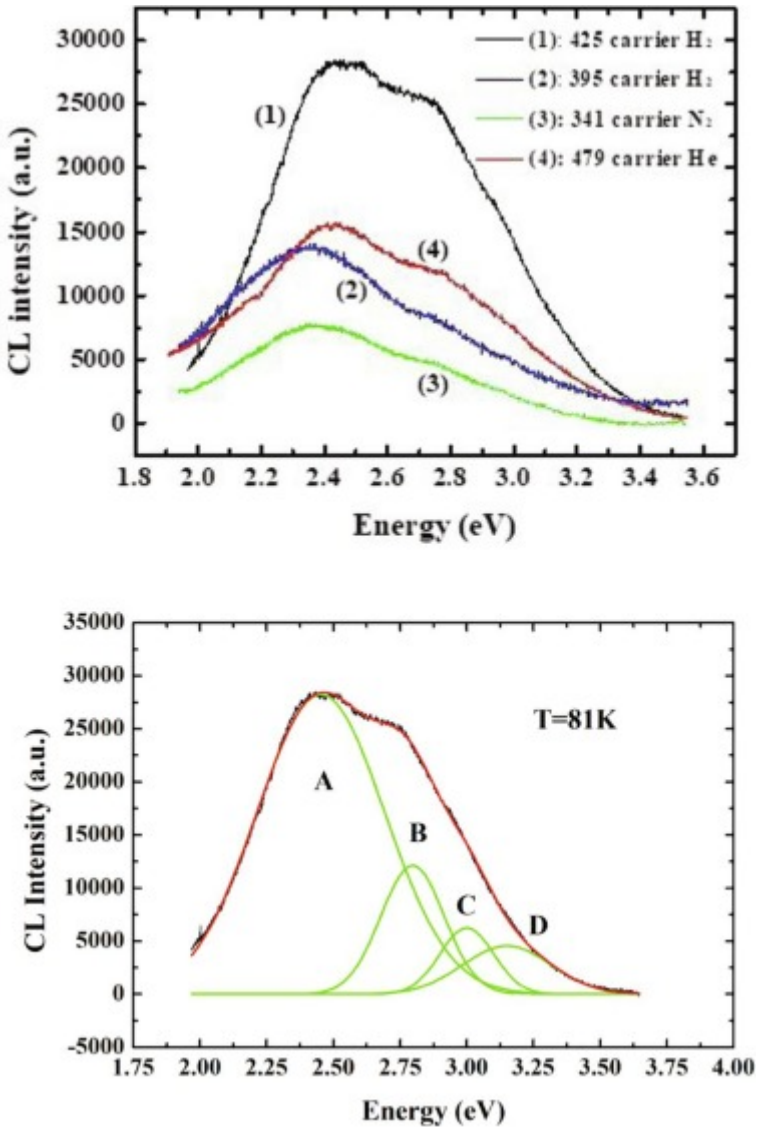

Fig. 2. a) CL spectra recorder at 81 K (electron beam: 30 KeV) for four undoped ε-Ga_2O_3 film grown under different process parameters (see list of samples in Table 1). T = 81 K. Note that sample #425 is more than 5 times thicker than the other three layers; the other samples have similar thickness (see Table 1). b) CL spectrum of the undoped ε-Ga_2O_3 film #425 of Fig. 2a at 81 K (black line, underlying) and best fit (red line, overlapped) performed by considering four Gaussian peaks (green lines).

All the recorded spectra from undoped films exhibited similar features, irrespective of the type of carrier gas, but presented remarkable differences in terms of the relative intensity of the peaks, as proved by repeating measurements on different samples. In order to have reliable data also for the thinnest ε-Ga_2O_3 specimen, where the sapphire substrate is also excited by the e-beam, the corresponding CL spectrum was "cleaned" by subtracting the CL spectrum of a reference c-oriented sapphire substrate, whose behavior vs. temperature in the range 2.2–4.5 eV is reported in Fig. S2 of Supplementary information. The CL spectrum of ε-Ga_2O_3 just lies in the energy

range where the CL spectrum of the substrate is negligible at any temperature, only showing a very slight bump around 2.2 eV and a peak at 3.7 eV.

Temperature dependent CL measurements were carried out (Fig. 3a) on the nominally undoped thick specimen in order to rule out any contribution from substrate. The possibility of using a high-energy electron beam permitted to detect a significant CL emission up to room temperature (RT). However, we must note that this sample had a RT resistivity of 1.5×10^4 Ωcm, at least 3 orders of magnitude lower than the typical resistivity (>10^7 Ωcm) of our nominally undoped samples [4]. Contamination by donors of unknown origin probably occurred in the less resistive sample analyzed here, which must be taken into account in the interpretation of the spectra. CL spectra were taken at stationary temperatures ranging from 80 K to 280 K, in steps of 10 K. Deconvolution of the temperature-dependent CL spectra confirms the presence of the four emission bands A, B, C and D with peak positions and FWHM practically unchanged over the whole temperature range. The integrated areas of the four peaks increase between 80 and 100 K, and then decrease monotonically between 100 K and 280 K (see Fig. 3b).

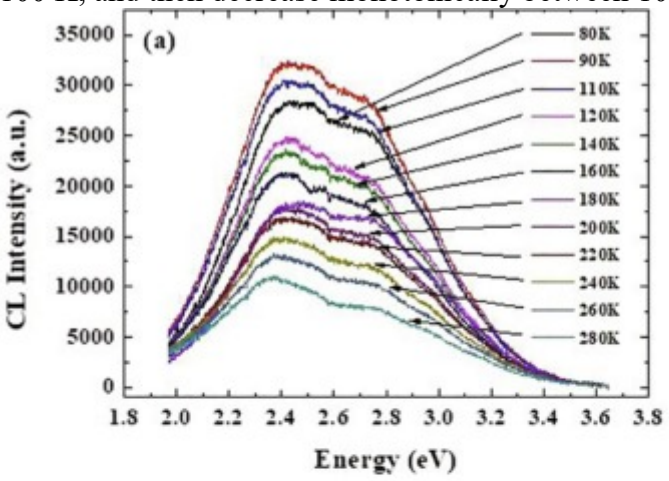

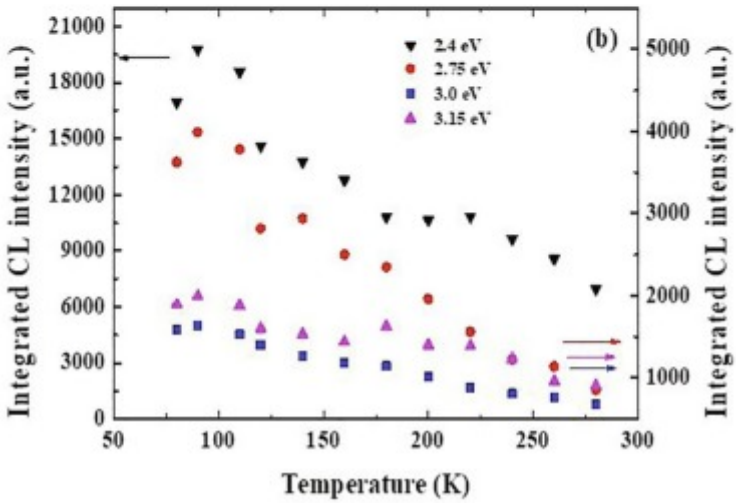

Fig. 3. Temperature dependence of: a) the CL spectra and b) the emission intensity of the A, B, C and D Gaussian peaks from 80 K to 280 K.

The slight increase of integrated areas of the four CL peaks when going from 80 to 100 K is attributed to thermal activation of electrons from shallow donor states to the conduction band, which strongly supports the hypothesis that the luminescence emissions involve the CB and four empty deep states. This hypothesis was also corroborated by previous photoconductivity (PC) investigations [4], as well as Angle Resolved Photo-Emission Spectroscopy (ARPES) by Mulazzi et al. [26]. Actually, the PC spectrum shows the onset of a weak signal well below the absorption edge of Ga_2O_3 (of about 2.4 eV), indicating that electrons are promoted into the CB from deep in-gap states by sub-bandgap excitation [4]. In addition, ARPES also suggested the emission of electrons from a band of deep states located about 1.1 eV above the valence band (VB) maximum [26]. These deep states are rather probably related to bulk defects, because no surface band bending was observed, which seems to rule out a significant concentration of surface states and related Fermi level pinning [26].

Above 100 K the emission intensity of the four bands monotonically decreases. The absence of the self-trapped exciton emission, and the thermal quenching of the deep level-related emissions are compatible with the transfer of the thermally-released holes to non-radiative recombination centers, according to the Schön-Klasens mechanism for thermal quenching [27].

Similar models were proposed by Binet et al. [21], and Onuma et al. [28] to justify the temperature dependence of the luminescence of β-Ga_2O_3. In β-phase, visible luminescence, in particular blue luminescence, was attributed to a donor-acceptor-pair transition (DAP), between a shallow donor level and a deep acceptor level. Initially, it was speculated that oxygen vacancies might act as shallow donors, but later calculations concluded that the vacancies must be deep donors with ionization energy above 1 eV [29]. Shallow donors in β-Ga_2O_3 samples seem to be associated with substitutional impurities in Ga sites [28], or Ga_i [30].

However, in the present ε-phase samples there is no blue shift associated with the thermal emptying of the shallow donor, which is consistent with the absence of DAP transitions, supporting the CB-deep level transitions. The actual physical picture is best described by the scheme of Fig. 4 although, at present, we cannot provide an unambiguous interpretation for the origin of the deep levels. In the more studied β-Ga_2O_3, deep levels have been tentatively attributed to V_{Ga} or $(Vo, V_{Ga})'$ complexes [31]. Actually, CL investigations performed on epitaxial β-Ga_2O_3 correlated specific CL emissions with intentionally-created defects: for instance, in Ref. [31] the blue

luminescence (3.5 eV) was associated with V_O; while bands A (2.4 eV), B (2.75 eV) and C (3 eV) have been connected with V_{Ga}-related defects [20], [31].

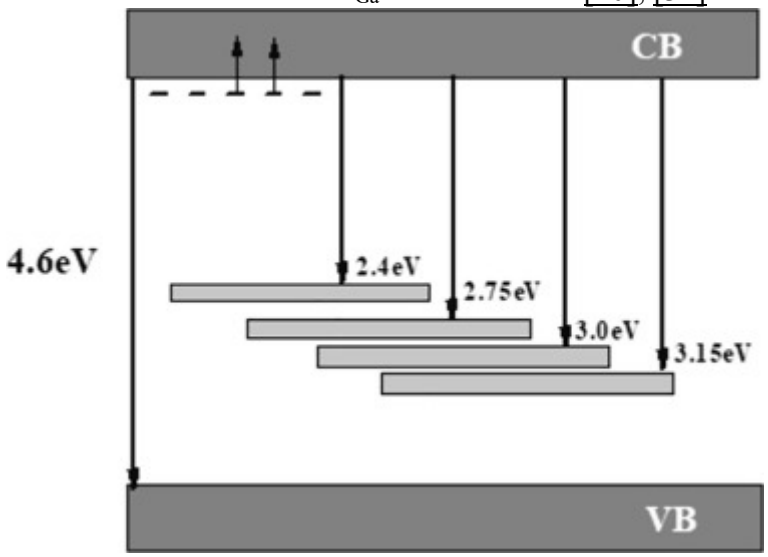

Fig. 4. Band diagram proposed for epsilon phase Ga_2O_3.

The detection of the same four peaks in all ε-Ga_2O_3 samples, although with different integrated areas, suggests that the deep defects responsible for the emissions are intrinsic, typical of our epitaxial process. However, the relative density of the defects is certainly dependent on the growth parameters, as proved by the change in the relative intensity of the associated emissions.

In order to investigate the role of Si-doping on the CL emission, two series of specimens with different silicon concentrations were grown using H_2 or N_2 as carrier gas. The main characteristics and growth parameters of these samples are listed in Table 1. CL spectra were seen to be strongly dependent on Si doping concentration, although the energy positions of the four peaks after deconvolution did not change with respect to the undoped samples.

Fig. 5a, b shows that the emission intensity drastically decreases with increasing Si concentration; furthermore, the integrated CL intensity was higher with hydrogen carrier gas than with nitrogen. However, the general CL trend as a function of the Si concentration was similar for both carrier gases (see also Fig. S3 of Supplementary information). On the other hand, it should be noted that the amount of silane that leads to almost complete quenching of the CL emission is significantly lower in the case of nitrogen carrier (see Fig. 6). All doped samples grown with hydrogen carrier have practically the same thickness therefore the intensity reduction can be ascribed without ambiguity to the increasing Si incorporation. The Si-doped samples grown with nitrogen carrier instead have different thicknesses; in particular, the heavier the doping

the higher the thickness, which implies that the intensity drop due to doping is somewhat mitigated by the larger excited crystal volume.

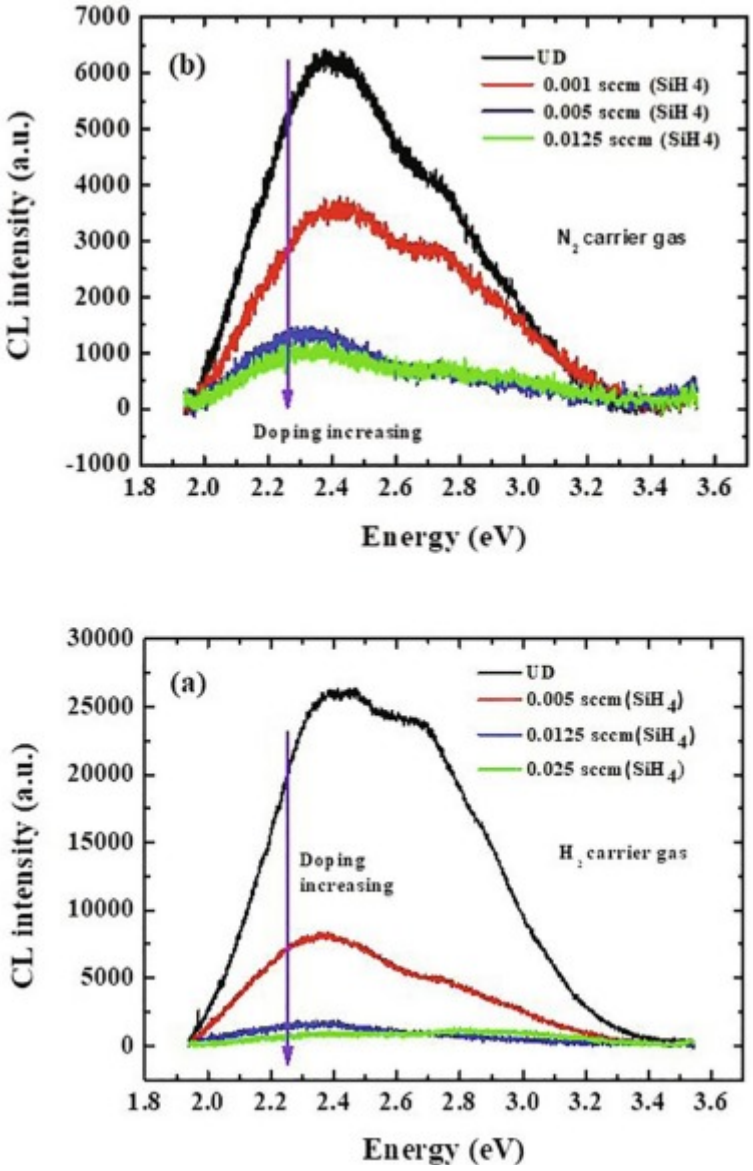

Fig. 5. CL spectra of samples grown with a) H_2 and b) N_2 carrier gas with different SiH_4 concentrations: the corresponding sccm are reported in the insert. The same spectra are reported in Supplementary Information plotted in semi-log scale to better evidence the relative intensities of all the emissions.

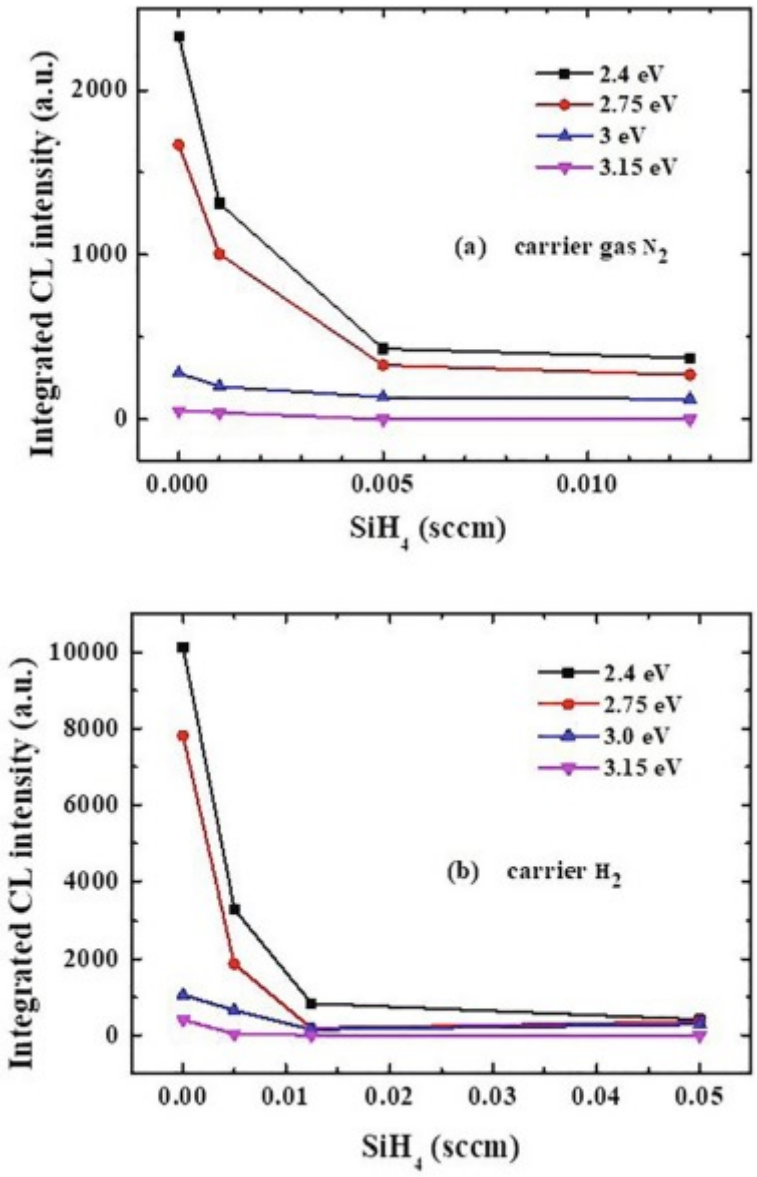

Fig. 6. Integrated CL intensity of the four peaks, after four-Gaussian deconvolution, vs SiH_4 flow with a) H_2 and b) N_2 carrier gas. No shift in energy of the peaks is observed as the doping concentration increases.

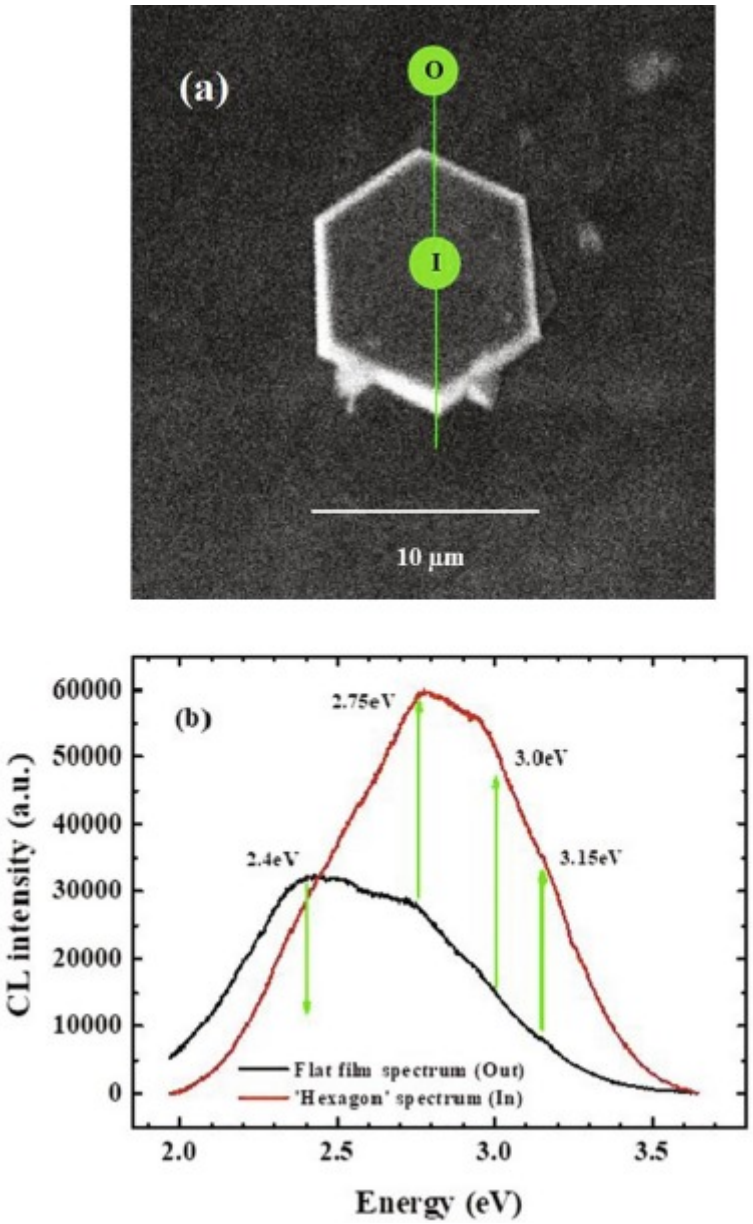

Fig. 7. a) Hexagonal surface crystal structure: spectral image of the CL emission, and b) CL spectra taken on flat film and on the 'hexagon', respectively, in the points O (Out) and I (In) along the green line indicated in the image of Fig. 7a.

Two qualitative conclusions can be drawn from the above results: i) the luminescence emission drops upon Si doping up to the almost complete quenching, but the rate of intensity decrease differs for each of the four deconvoluted peaks; ii) nitrogen as carrier gas reduces itself the overall CL intensity. Let us consider for example the spectra of the two samples doped with silane flux of 0.005 sccm in Fig. 5a and b: the sample in H_2 exhibits a CL intensity about eight times higher than the sample in N_2, which cannot be accounted for by the thickness difference.

The decrease in the overall CL emission with Si doping in films grown under H_2 carrier could be tentatively attributed to formation of Si-related non-radiative killer centers or

to reduction of the concentration of deep complex acceptors responsible for the A-D transitions or to both effects acting simultaneously. One idea is that the A-D acceptors involve Ga vacancies + other unidentified point defects [32]. Actually, it has been demonstrated that Si in tetrahedral Ga site behaves as a simple shallow donor [15], [24] but there is no information about the behavior of Ga-vacancy complexes partially saturated by Si.

In the case of films deposited under N_2 (Fig. 5b) the picture is even more complicated. Generally, ε-Ga_2O_3 films with the same nominal Si content were actually less conductive when nitrogen was used as carrier gas instead of hydrogen. Nitrogen was indeed reported to be a deep acceptor in β gallium oxide [32], [34], [35] and in principle it could be a deep acceptor also in ε-Ga_2O_3, however, the fact that the same deep level transitions are seen in both, H_2 and N_2, samples rules out the role of nitrogen as a deep acceptor participating in the luminescence emission; it might be associated with a non-radiative recombination center, accounting for the lower emission efficiency of the N_2-carrier samples. On the other hand, also the possible formation of deep donor complexes involving interstitial-substitutional nitrogen, $(N_2)_{Ga}$, $(N_2)_O$ should be taken into account to evaluate the effect of nitrogen incorporation on the sample resistivity [36]. More investigation is clearly necessary in order to provide a reliable interpretation for the electrical data of ε-Ga_2O_3.

Nitrogen incorporated as deep acceptor in ε-Ga_2O_3 could also justify the lower CL intensity, observed both in undoped and Si-doped films of Fig. 5b, with respect to films grown in H_2 ambient. The N_2-related deep level could shift the Fermi level position, and thus modify the occupancy of other acceptor levels (A-D) and relevant hole trapping processes. Under this hypothesis, the lower CL intensity would derive, first, from nitrogen-related centers and, secondly, from the annihilation of V_{Ga}-related defects consequent to Si doping. For sake of completeness, it must be mentioned here that previous positron annihilation spectroscopy in β phase [33] surprisingly reported an increase of Ga vacancies with Si-doping, which would clash with our model of deep acceptor annihilation.

Spectrally integrated CL intensities of the four A-D peaks are shown in Fig. 6a and b: in both series of samples, with either hydrogen or nitrogen carrier gas, the different peaks are seen to react differently to Si doping. Moreover, nitrogen seems to enhance the 2.4 eV (517 nm) band with respect to the other bands, which supports the idea that nitrogen incorporation really changes the charge balance between deep levels.

It can thus be concluded that in Si-doped samples grown with H_2 carrier, the different intensity decrease rate of the four CL peaks up to complete luminescence quenching can be explained by two phenomena: creation of non-radiative recombination centers and strong decrease of deep levels concentrations at different rates. In less conductive Si-doped samples grown with N_2 carrier there is also an additional effect due to nitrogen-related deep acceptors, which would behave as non-radiative recombination centers and also would shift the Fermi level balancing the occupancy of the deep levels responsible for the luminescence emission.

Finally, the analysis of the CL emission from some peculiar surface features provides some hints about the relation between growth mode and the formation of deep energy states. During the growth of ε-Ga_2O_3 hexagonal islands form and expand laterally [18]; one of such islands is shown in Fig. 7a. From the shape of the island, it is likely that the lateral expansion of the island is much faster than the vertical growth on the film surface external to the hexagon.

Comparison of the CL spectra taken on the hexagon and on the flat surface around it reveals that the 2.75 eV, 3.0 and 3.15 eV bands (namely B, C and D, see Fig. 7b), are strongly enhanced within the micrometric hexagonal island whereas, as clearly shown in Fig. 7b, the emission A at 2.4 eV dominates outside the island. Unfortunately, a microscopic picture of the individual point/complex defects responsible for the four CL emissions is still missing, but it may be argued, in analogy with what is observed in β-Ga_2O_3, that in these surface islands the complexes including gallium vacancies (V_{Ga}) [31] are present in higher concentration with respect to the outside region. The lateral expansion rate of the island is certainly higher than the normal growth rate on the rest of the film surface, which in turn means higher probability of incorporating point defects, namely Ga vacancies and related complexes. These observations further support the idea of deep acceptor states linked to intrinsic stoichiometric defects.

4. Conclusions

Low-temperature CL spectra were taken on nominally undoped and Si-doped ε-Ga_2O_3 samples in order to investigate the deep levels in the bandgap. Undoped samples were grown by MOVPE on (0001)-Al_2O_3 substrates, using different carrier gases: He, H_2 or N_2. Si-doping was performed with either H_2 or N_2 carrier gas. No band-to-band emission was observed, however a broad CL emission covering the 2–3.4 eV photon energy range was detected in all the samples. We attributed this band to convolution of four narrower Gaussian bands peaked at about 2.4 (A), 2.75 (B), 3.0 (C) and 3.15 eV

(D). The intensity of the individual bands was observed to decrease significantly with measurement temperature as well as Si doping concentration. Generally, a strong reduction of the CL integrated emission occurs even for relatively low Si addition. The overall CL data were interpreted as due to transitions from the CB to deep acceptors, probably the same states detected by previous ARPES investigation on similar samples. In analogy with the results previously reported for the β phase, we are inclined to link the acceptor states with intrinsic point defects. Gallium vacancies in particular seem to play a fundamental role, as also suggested by looking at the intensity of the four peaks in surface growth islands that grow laterally at a rate higher than the vertical rate of the remaining film surface. Different growth rate actually implies different incorporation of point defects.

Acknowledgements

The authors wish to thank Prof. Maura Pavesi, Prof. Andrea Baraldi and Prof. Alessio Bosio of the Department of Mathematical, Physical, and Computer Sciences, University of Parma, for useful discussions. S. Dadgostar, and J. Jimenez were funded by Junta de Castilla y Leon (project VA283P18).

References

1. M. Higashiwaki, K. Sasaki, T. Kamimura, M.H. Wong, D. Krishnamurthy, A. Kuramata , T. Masui, S. Yamakoshi; Depletion-mode Ga_2O_3 metal-oxide-semiconductor field-effect transistors on β-Ga_2O_3 (010) substrates and temperature dependence of their device characteristics; Appl. Phys. Lett., 103 (2013), Article 123511
2. M. Oda, R. Tokuda, H. Kambara, T. Tanikawa, T. Sasaki, T. Hitora; Schottky barrier diodes of corundum-structured gallium oxide showing on-resistance of 0.1 mΩ·cm2 grown by MIST EPITAXY; Appl. Phys. Express, 9 (2016), Article 021101
3. M. Higashiwaki, K. Sasaki, H. Murakami, Y. Kumagai, A. Koukitu, A. Kuramata, T. M asui, S. Yamakoshi; Recent progress in Ga_2O_3 power devices; Semicond. Sci. Technol., 31 (2016), Article 034001
4. M. Pavesi, F. Fabbri, F. Boschi, G. Piacentini, A. Baraldi, M. Bosi, E. Gombia, A. Paris ini, R. Fornari; ε-Ga_2O_3 epilayers as a material for solar-blind UV photodetectors Mater. Chem. Phys., 205 (2018), p. 502
5. D. Guo, Z. Wu, P. Li, Y. An, H. Liu, X. Guo, H. Yan, G. Wang, C. Sun, L. Li, W. Tang Fabrication of β-Ga_2O_3 thin films and solar-blind photodetectors by laser MBE technology; Opt. Mater. Express, 4 (2014), p. 1067
6. M. Zhong, Z. Wei, X. Meng, F. Wu, J. Li; High-performance single crystalline UV photodetectors of β-Ga_2O_3; J. Alloys Compd., 619 (2015), p. 572
7. Y. Kokubun, K. Miura, F. Endo, S. Nakagomi; Sol-gel prepared β-Ga_2O_3 thin films for ultraviolet photodetectors; Appl. Phys. Lett., 90 (2007), Article 031912
8. S.J. Pearton, J. Yang, P.H. Cary, F. Ren, J. Kim, M.J. Tadjer, M.A. Mastro; A review of Ga_2O_3 materials, processing, and devices; Appl. Phys. Rev., 5 (2018), Article 011301

9. Y. Tomm, P. Reiche, D. Klimm, T. Fukuda; Czochralski grown Ga_2O_3 crystalsJ. Cryst. Growth, 220 (2000), p. 510
10. Kuramata, K. Koshi, S. Watanabe, Y. Yamaoka, T. Masui, S. Yamakoshi High-quality β-Ga_2O_3 single crystals grown by edge-definedfilm-fed growth Jpn. J. Appl. Phys., 55 (2016), p. 1202A2
11. Z. Galazka, K. Irmscher, R. Uecker, R. Bertram, M. Pietsch, A. Kwasniewski, M. Neum ann, T. Schulz, R. Schewski, D. Klimm, M. Bickermann; On the bulk β-Ga_2O_3 single crystals grown by the Czochralski method; J. Cryst. Growth, 404 (2014), p. 184
12. F. Ricci, F. Boschi, A. Baraldi, A. Filippetti, M. Higashiwaki, A. Kuramata, V. Fiorenti ni, R. Fornari; J. Phys.: Condens. Matter, 28 (2016), Article 224005
13. Cora, F. Mezzadri, F. Boschi, M. Bosi, M. Čaplovičová, G. Calestani, I. Dódon, B. Pécz , R. Fornari; The real structure of ε-Ga_2O_3 and its relation to κ-phase; Cryst. Eng. Commun., 19 (2017), p. 1509
14. R. Fornari, M. Pavesi, V. Montedoro, D. Klimm, F. Mezzadri, I. Cora, B. Pecz, F. Bosc hi, A. Parisini, A. Baraldi, C. Ferrari, E. Gombia, M. Bosi; Thermal stability of ε-Ga_2O_3 polymorph; Acta Mater., 140 (2017), p. 411
15. Parisini, A. Bosio, V. Montedoro, A. Gorreri, A. Lamperti, M. Bosi, G. Garulli, S. Vant aggio, R. Fornari; Si and Sn doping of ε-Ga_2O_3 layers; APL Mater., 7 (2019), Article 031114
16. F. Mezzadri, G. Calestani, F. Boschi, D. Delmonte, M. Bosi, R. Fornari; Crystal structure and ferroelectric properties of ε-Ga_2O_3 films grown on (0001)-sapphire Inorg. Chem., 55 (2016), p. 12079
17. Y. Oshima, E.G. Víllora, Y. Matsushita, S. Yamamoto, K. Shimamura; Epitaxial growth of phase-pure ε- Ga_2O_3 by halide vapor phase epitaxy; Appl. Phys., 118 (2015), Article 085301
18. F. Boschi, M. Bosi, T. Berzina, E. Buffagni, C. Ferrari, R. Fornari; Hetero-epitaxy of ε-Ga_2O_3 layers by MOCVD and ALD; Cryst. Growth, 443 (2016), p. 25
19. E.G. Víllora, T. Atou, T. Sekiguchi, T. Sugawara, M. Kikuchi, T. Fukuda Cathodoluminescence of undoped β-Ga_2O_3 single crystals; Solid State Commun., 120 (2001), p. 455
20. T. Onuma, S. Fujioka, T. Yamaguchi, M. Higashiwaki, K. Sasaki, T. Masui, T. Honda Correlation between blue luminescence intensity and resistivity in β-Ga_2O_3 single crystals; Appl. Phys. Lett., 103 (2013), Article 041910
21. Binet, D. Gourier; Origin of the blue luminescence of β-Ga_2O_3; J. Phys. Chem. Solids, 59 (1998), p. 1241
22. Z. Zhang, E. Farzana, A.R. Arehart, S.A. Ringel; Deep level defects throughout the bandgap of (010) β-Ga_2O_3 detected by optically and thermally stimulated defect spectroscopy; Appl. Phys. Lett., 108 (2016), Article 052105[23]
23. E. Farzana, M.F. Chaiken, T.E. Blue, A.R. Arehart, S.A. Ringel; Impact of deep level defects induced by high energy neutron radiation in β-Ga_2O_3; APL Mater., 7 (2019), Article 022502
24. H.J. von Bardeleben, J.L. Cantin, A. Parisini, A. Bosio, R. Fornari; Conduction mechanism and shallow donor properties in silicon-doped ε- Ga_2O_3 thin films: an electron paramagnetic resonance study“ Phys. Rev. Mater., 3 (2019), Article 084601
25. D. Drouin, A.R. Coutre, R. Gauvin, P. Hovington, P. Horny, H. Demers, Montecarlo simulation of electron trajectories in solids (CASINO), University of Sherbrooke, Quebec, Canada, http://www.gel.usherbrooke.ca/casino/What.html.
26. Mulazzi, F. Reichmann, A. Becker, W.M. Klesse, P. Alippi, V. Fiorentini, A. Parisini, M. Bosi, R. Fornari; The electronic structure of ε-Ga_2O_3; APL Mater., 7 (2019), Article 022522

27. M.A. Reshchikov; Temperature dependence of defect-related photoluminescence in III-V and II-VI semiconductors; J. Appl. Phys., 115 (2014), Article 012010
28. T. Onuma, Y. Nakata, K. Sasaki, T. Masui, T. Yamaguchi, T. Honda, A. Kuramata, S. Yamakoshi, M. Higashiwaki; Modeling and interpretation of UV and blue luminescence intensity in β-Ga_2O_3 by silicon and nitrogen doping; J. Appl. Phys., 124 (2018), Article 075103
29. J.B. Varley, J.R. Weber, A. Janotti, C.G. Van de Walle; Oxygen vacancies and donor impurities in β-Ga_2O_3; Appl. Phys. Lett., 97 (2010), Article 142106
30. P. Deak, Q.D. Ho, F. Seemann, B. Aradi, M. Lorke, T. Frauenheim; Choosing the correct hybrid for defect calculations: a case study on intrinsic carrier trapping in β-Ga_2O_3; Phys. Rev. B, 95 (2017), Article 075208
31. H. Gao, S. Muralidharan, N. Pronin, M.R. Karim, S.M. White, T. Asel, G. Foster, S. Kr shnamoorthy, S. Rajan, L.R. Cao, M. Higashiwaki, H. vonWenckstern, M. Grundmann, H. Zhao, D.C. Look, L.J. Brillson; Optical signatures of deep level defects in Ga_2O_3 Appl. Phys. Lett., 112 (2018), Article 242102
32. Stephan Lany; Defect phase diagram for doping of Ga_2O_3; APL Mater., 6 (2018), Article 046103
33. E. Korhonen, F. Tuomisto, D. Gogova, G. Wagner, M. Baldini, Z. Galazka, R. Schewsk i, M. Albrecht; Electrical compensation by Ga vacancies in Ga_2O_3 thin films; Appl. Phys. Lett., 106 (2015), Article 242103
34. M.J. Tadjer, A.D. Koehler, J.A. Freitas Jr., J.C. Gallagher, M.C. Specht, E.R. Glaser, K. D. Hobart, T.J. Anderson, F.J. Kub, Q.T. Thieu, K. Sasaki, D. Wakimoto, K. Goto, S. Watanabe, A. Kuramata; High resistivity halide vapor phase homoepitaxial β-Ga_2O_3 films co-doped by silicon and nitrogen; Appl. Phys. Lett., 113 (2018), Article 192102
35. J.L. Lyons; A survey of acceptor dopants for β-Ga_2O_3; Semicond. Sci. Technol., 33 (2018), p. 05LT02
36. H. Peelaers, J.L. Lyons, J.B. Varley, C.G. Van de Walle; Deep acceptors and their diffusion in Ga_2O_3; APL Mater., 7 (2019), Article 022519